

A-TDOM: Active TDOM via On-the-Fly 3DGS

Yiwei Xu, Xiang Wang, Yifei Yu, Wentian Gan, Luca Morelli, Giulio Perda, Xiongwu Xiao, Zongqian Zhan, Xin Wang, and Fabio Remondino

Abstract—True Digital Orthophoto Map (TDOM) serves as a crucial geospatial product in various fields such as urban management, city planning, land surveying, etc. However, traditional TDOM generation methods generally rely on a complex offline photogrammetric pipeline, resulting in delays that hinder real-time applications. Moreover, the quality of TDOM may degrade due to various challenges, such as inaccurate camera poses or Digital Surface Model (DSM) and scene occlusions. To address these challenges, this work introduces A-TDOM, a near real-time TDOM generation method based on On-the-Fly 3DGS optimization. As each image is acquired, its pose and sparse point cloud are computed via On-the-Fly SfM. Then new Gaussians are integrated and optimized into previously unseen or coarsely reconstructed regions. By integrating with orthogonal splatting, A-TDOM can render just after each update of a new 3DGS field. Initial experiments on multiple benchmarks show that the proposed A-TDOM is capable of actively rendering TDOM in near real-time, with 3DGS optimization for each new image in seconds while maintaining acceptable rendering quality and TDOM geometric accuracy.

Index Terms—TDOM, On-the-Fly SfM, 3DGS, UAV Images.

I. INTRODUCTION

Aerial True Digital Orthophoto Map (TDOM) features high resolution and rich texture information, making it widely applied in various fields (e.g., digital twin, city planning, etc.). Compared to the Digital Orthophoto Map (DOM), TDOM needs occlusion detection to avoid noticeable tilting or distortion. However, most traditional TDOM generation methods rely on DSM for occlusion detection (e.g.,

This work was supported by the National Natural Science Foundation of China (No. 42301507). (Corresponding author: Xin Wang, xwang@sgg.whu.edu.cn)

Yiwei Xu, Xiang Wang, Yifei Yu, Wentian Gan, Zongqian Zhan and Xin Wang are with the School of Geodesy and Geomatics, Wuhan University, Wuhan, 430079, China. Xiongwu Xiao are with the State Key Laboratory of Information Engineering in Surveying, Mapping and Remote Sensing (LIESMARS), Wuhan University, Wuhan, 430072, China. Luca Morelli, Giulio Perda and Fabio Remondino are with 3D Optical Metrology (3DOM) Unit, Bruno Kessler Foundation (FBK), 38123, Trento, Italy.

Prof. Dr.-Ing. Xin Wang obtained his PhD from Leibniz University Hannover, Germany in 2021, and has published over 20 scientific papers in the topic of processing UAV images for generating DEM, DSM, DOM, etc., he is now the editor of two well-known photogrammetric Journals - The PFG Journal, and Photogrammetric Engineering & Remote sensing.

Prof. Zongqian Zhan is a full professor at Wuhan University. He has nearly 30-year experience in the field of UAV photogrammetry, with nearly 50 scientific papers that are basically relevant to photogrammetric tasks using UAV images; In addition, he is also very active in the industry field and serves for over 95 percent relevant markets in China.

Prof. Fabio Remondino is a leading authority in UAV photogrammetry, with core expertise in automated 3D modeling and data processing from unmanned platforms. His impactful research, evidenced by nearly 27k citations with one paper on UAV 3D mapping alone over 2.2k citations (Google Scholar), has significantly advanced UAV applications in cultural heritage and environmental monitoring. He previously chaired the ISPRS Commission II “Photogrammetry” (2016-2022) and conferences related to UAVs, leading international efforts to standardize and innovate in the field.

Comprehensive details regarding the co-authors’ relevant expertise and past activities are available on their individual webpages.

Z-buffering [1]), which is computationally expensive. In recent years, learning-based methods have been proposed on TDOM generation. Several NeRF-based methods have achieved TDOM generation by employing orthogonal volume rendering techniques [2]. Furthermore, recent work has increasingly explored 3D Gaussian Splatting (3DGS) [3] for TDOM generation. Tortho-Gaussian [4] utilizes fully anisotropic Gaussian kernels and Orthogonal Splatting to render TDOM. Yang et al. introduced Ortho-3DGS [5], which integrates depth information to enhance the reconstruction of the Gaussian field and further proposed a True Orthographic Rasterization Rendering method tailored for TDOM generation. These 3DGS-based methods are capable of producing high-quality TDOM without DSM and occlusion detection, representing a significant improvement over the traditional pipeline.

However, most existing methods still employ offline processing after the acquisition of all images, limiting the potential of real-time applications. There are few works for real-time DOM generation [6]–[8], but not for TDOM. To counter these limitations, this paper presents A-TDOM, a workflow which enables simultaneous image acquisition and active TDOM generation based on 3DGS. In summary, this work makes the following contributions:

- A-TDOM, a workflow to enable robust online active TDOM generation without DSM and occlusion detection. To the best of our knowledge, it is the first attempt to generate TDOM in near real-time.
- A near real-time 3DGS optimization, based on Gaussians Sampling and Integration method to novelly update the current 3DGS field for each new image. Subsequently, several adaptive optimization strategies are proposed to accelerate the optimization for previously unseen regions.
- An innovative approach, based on projection matrix modification, to enable orthographic splatting and obtain TDOM from 3DGS.“

II. PRELIMINARY

Zhan et al. proposed On-the-Fly SfMv2 [9] (See more at <https://yifeiyu225.github.io/on-the-flySfMv2.github.io/>), achieving near real-time pose estimation and sparse point cloud during image capturing. It employs a Hierarchical Weighted Local Bundle Adjustment for efficient refinement and uses global feature retrieval and HNSW for online matching, enabling real-time updates for the image matching matrix. This paper is built on the On-the-Fly SfM to update poses and sparse point cloud for our subsequent A-TDOM.

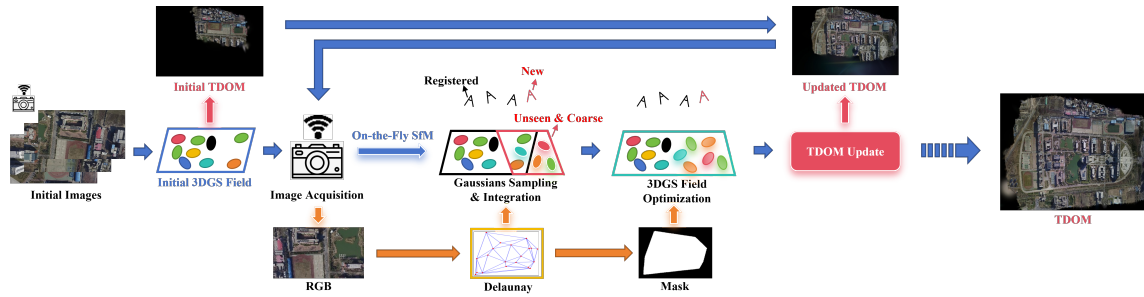


Fig. 1. The A-TDOM workflow: after an initial 3DGS field, for each new image, a Delaunay triangulation is applied to create a mask for 3DGS field updating and optimization. A-TDOM is generated after each 3DGS field update via orthogonal splatting.

III. METHODOLOGY

A. Overview of A-TDOM

To generate active TDOM (a-TDOM) in near real-time, we propose a progressive online 3DGS optimization framework. As illustrated in Fig. 1, it begins by training an initial 3DGS field. Then, as each new image arrives, we perform the following steps: 1) Pose refinement for both newly acquired and registered images while updating the sparse point cloud using On-the-Fly SfM. 2) Delaunay triangulation on each image plane based on reprojection of sparse point cloud, the subsequent 3DGS optimization is constrained by triangular coverage regions. 3) A novel Gaussian Sampling and Integration method is employed to replace the densification in the original 3DGS, only necessary Gaussians are appended into the current 3DGS field. 4) Optimization of 3DGS field is performed after each Gaussian Sampling and Integration, followed by TDOM generation through orthogonal splatting.

B. Key Region Determination via Reprojected Delaunay Triangulation Masking

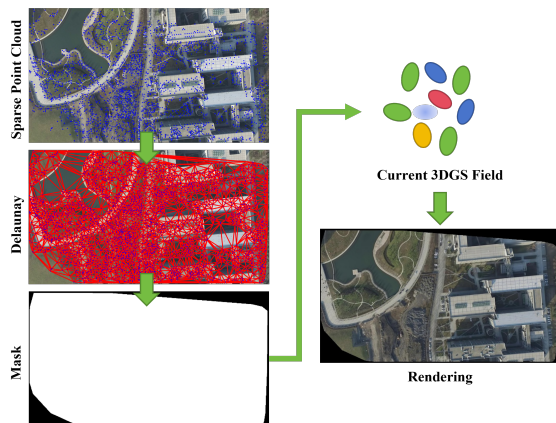


Fig. 2. Scene reconstruction based on Delaunay triangular masking. The goal is to ensure that regions with sufficient overlap are optimized.

Traditional TDOM methods typically consider regions with sufficient image overlap, while areas with low overlap (e.g., scene boundaries) are excluded from generated TDOM. On the other hand, the 3DGS training aims to minimize the rendering loss across all images, potentially leading to the reconstruction of regions visible to only single image with insufficient overlap, which is not the most optimal.

To address this, we estimate the key region based on the visibility between sparse point cloud and each image. As illustrated in Fig. 2, for each input image, we reproject the sparse point cloud of on-the-fly SfM onto this image plane and the visible reprojections are applied using Delaunay triangulation, followed by forming a mask based on the triangulated area. In the subsequent 3DGS optimization, only the masked image region which can ensure sufficient overlap is optimized, while regions with insufficient overlap are excluded from training.

C. Gaussians Sampling and Integration

To address the uncontrollability of the original 3DGS densification strategy that impedes online training, we propose a novel Gaussian Sampling and Integration method for online 3DGS field expansion. As illustrated in Fig. 3, for each new image, its pose and updated the sparse point cloud are computed via On-the-Fly SfM. Then, the corresponding masked key region is determined, within which, we render the content using the current 3DGS field and compute the gradient map using the Laplacian of Gaussian (LoG) operator. Similarly, the gradient map of the input image itself is computed. By subtracting these two gradient maps, it is possible to identify pixels with a gradient discrepancy exceeding a predefined threshold G_m , which are selected as regions that require additional Gaussians integration.

After selecting the regions R_a with additional Gaussians integration, we sample the new Gaussians with positions and colors. First, we uniformly sample H_t points within each Delaunay triangle and extract all sampled points that fall within the region R_a . Subsequently, all the sampled points are mapped into 3D space. More specifically, assume a sampled point $s(x_s, y_s)$ locates in the triangle τ , whose vertices' 2D coordinates are $p_{\tau_1}(x_1, y_1)$, $p_{\tau_2}(x_2, y_2)$ and $p_{\tau_3}(x_3, y_3)$, and the corresponding 3D coordinates are $P_{\tau_1}(X_1, Y_1, Z_1)$, $P_{\tau_2}(X_2, Y_2, Z_2)$ and $P_{\tau_3}(X_3, Y_3, Z_3)$. The 3D coordinate $P_S(X_s, Y_s, Z_s)$ of the sampled point is approximated as follows:

$$\lambda_1 = \frac{(y_2 - y_3)(x_s - x_3) + (x_3 - x_2)(y_s - y_3)}{(y_2 - y_3)(x_1 - x_3) + (x_3 - x_2)(y_1 - y_3)} \quad (1)$$

$$\lambda_2 = \frac{(y_3 - y_1)(x_s - x_3) + (x_1 - x_3)(y_s - y_3)}{(y_2 - y_3)(x_1 - x_3) + (x_3 - x_2)(y_1 - y_3)} \quad (2)$$

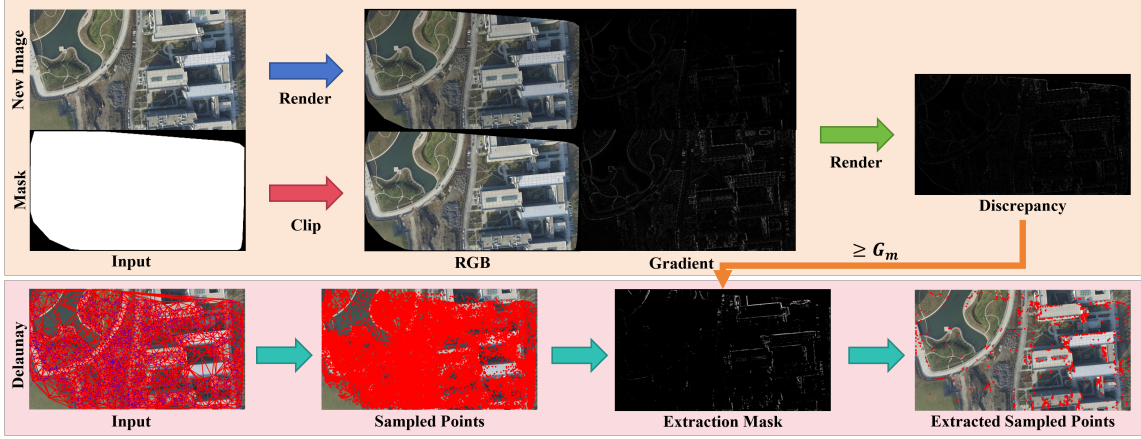


Fig. 3. Gaussians Sampling and Integration. We identify previously unseen and coarsely reconstructed region depends on gradient discrepancy map, and generate the extraction mask. Subsequently, we sample points for Gaussians integration.

$$\lambda_3 = 1 - \lambda_1 - \lambda_2 \quad (3)$$

$$P_S = \lambda_1 P_{\tau_1} + \lambda_2 P_{\tau_2} + \lambda_3 P_{\tau_3} \quad (4)$$

Similarly, assuming the colors of the triangle vertices are C_{τ_1} , C_{τ_2} and C_{τ_3} , the color C_S of the sampled point is initialized as follows:

$$C_S = \lambda_1 C_{\tau_1} + \lambda_2 C_{\tau_2} + \lambda_3 C_{\tau_3} \quad (5)$$

After estimating the 3D coordinates and colors of all sampled points, new Gaussians are integrated into the current 3DGS field based on this information, subsequently 3DGS optimization is performed.

D. Adaptive 3DGS Optimization Strategies

Inspired by previous Gaussian On-the-Fly Splatting [10], several modifications are applied to the original 3DGS training strategies, including Adaptive Learning Rate Update and Local Optimization, which assign learning rates per image and allocate more training iterations to newly acquired images, supporting online 3DGS optimization.

E. Orthographic Splatting for TDOM Generation

To eliminate building facades and fulfill the basic requirement of TDOM, both the mean and covariance of 3D Gaussians undergo orthographic projection. For the mean, the orthogonal projection matrix P_o is defined as:

$$P_o = \begin{pmatrix} \frac{2}{r-l} & 0 & 0 & -\frac{r+l}{l-u} \\ 0 & \frac{2}{r-u} & 0 & -\frac{t+b}{l-u} \\ 0 & 0 & \frac{2}{z_l-z_n} & \frac{z_l+z_n}{z_l-z_n} \\ 0 & 0 & 0 & 1 \end{pmatrix} \quad (6)$$

This matrix maps world coordinates into an orthogonal clip space bounded by the parameters l, r, b, t, z_n, z_f , corresponding to the left, right, bottom, top, near, and far planes of the viewing box. For the covariance, we linearly approximate its effect using the following Jacobian matrix:

$$\Sigma' = J \Sigma J^T \quad (7)$$

$$J = \begin{pmatrix} \frac{2}{r-l} & 0 & 0 \\ 0 & \frac{2}{t-b} & 0 \\ 0 & 0 & 0 \end{pmatrix} \quad (8)$$

Note that this orthographic splatting can be executed very fast using the original rasterization technique.

IV. EXPERIMENT AND DISCUSSION

To validate the efficacy of the proposed A-TDOM, several NPU DroneMap dataset [11] and one self-generated dataset are tested. For each dataset, we first perform 2000 training iterations for the initial 3DGS generation. After new image comes in, we set the gradient discrepancy threshold $G_m = 0.1$ to sample and integrate new Gaussians for 3DGS field expansion. Then, 200 optimization iterations are performed on the current 3DGS field, and the TDOM is updated once the new optimization is completed. All other settings are consistent with the original 3DGS configuration.

As Fig. 4 shows, our method is compared with two offline 3DGS-based methods (Tortho-Gaussian and AdR-Gaussian) and three commercial software (ContextCapture, Metashape, and Pix4DMapper) across three scenarios: building edge, building facade, and slender structure. For comparison, the full resolution of input images is employed, and the generated TDOMs are with identical resolution.

Building Edge: Both Tortho and AdR methods exhibit blurred edge delineation, and three commercial software demonstrate significant distortion and serrated edge. In contrast, our method maintains complete structure, achieving sharper edge definition.

Building Facade: Three commercial software exhibit the outer wall, displaying pronounced perspective displacement, while ours effectively removes building facades.

Slender Structure: The red box highlights instances of blurring, distortion, and discontinuities in comparative methods, whereas our A-TDOM preserves geometric continuity and structural fidelity.

TABLE I
TIME EFFICIENCY COMPARISON OF TDOMS GENERATION

Scene	ImageNum	3DGS-based methods					Commercial softwares		
		Pose estimation (s)	Ours-FPS	Ours	Ad-opt time (s)		Total time (s)		
					Tortho-GS	AdR-GS	ContextCapture	MetaShape	Pix4DMapper
phantom3-npu	300	568	0.53	78	874	1803	1398	2533	1601
phantom3-ieue	399	818	0.49	83	848	1860	1278	2583	1443
WHU-S	242	668	0.36	111	769	1705	4164	2038	816
WHU-Q1	248	367	0.68	58	669	1701	1291	1741	487

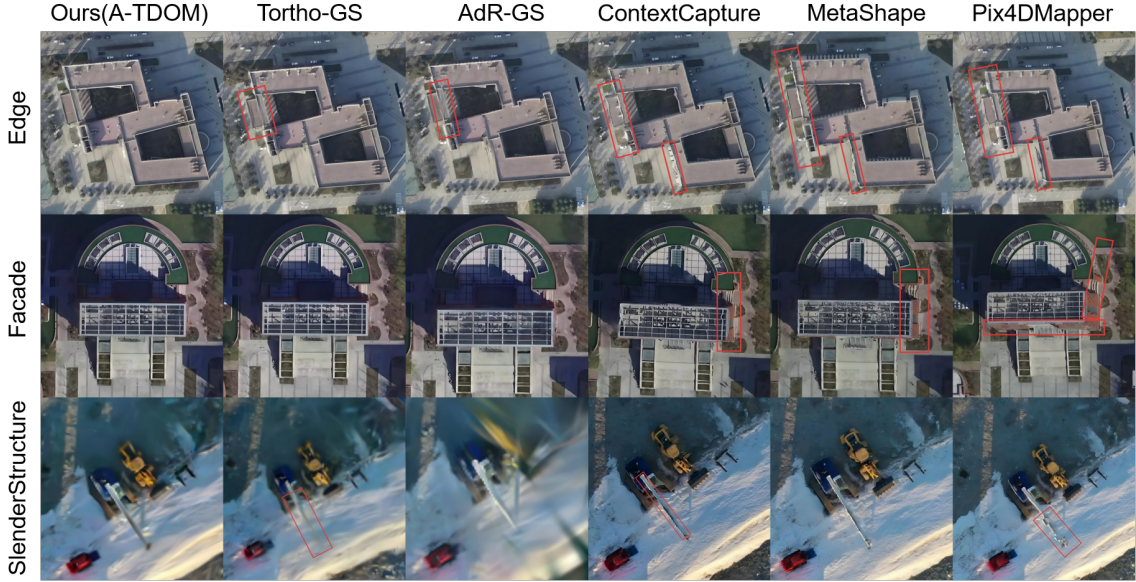


Fig. 4. Qualitative comparison of TDOMs generated by A-TDOM, 3DGS-based methods and commercial software on various scenes.

Time Efficiency: For 3DGS-based methods, we record the cost time of pose estimation by On-the-Fly SfM and estimate the FPS of our A-TDOM. Additionally, we record the cost time from the completion of pose estimation to the completion of 3DGS field optimization and final TDOM generation (Ad-Opt time). For the commercial software, we record the total time from pose estimation to TDOM generation, which corresponds to the sum of the pose estimation time and the Ad-opt time in 3DGS-based methods. As illustrated in Table I, A-TDOM achieves a significant advantage over other 3DGS-based methods and commercial software.

V. CONCLUSION

The paper proposes A-TDOM, a near real-time TDOM generation method via On-the-Fly 3DGS optimization. We employ a novel Gaussians Sampling and Integration method, modifying the training strategies of origin 3DGS optimization, substituting the perspective projection with orthogonal projection, enabling near real-time TDOM generation while drone images are captured.

REFERENCES

- [1] K. UCHIDA and T. DOIHARA, "Triangle-based visibility analysis and true orthoimage generation," *Int. Arch. Photogramm. Remote Sens. Spatial Inf. Sci.*, 2004.
- [2] J. Wei, G. Zhu, and X. Chen, "Nerf-based large-scale urban true digital orthophoto map generation method," *IEEE Journal of Selected Topics in Applied Earth Observations and Remote Sensing*, 2024.
- [3] B. Kerbl, G. Kopanas, T. Leimkühler, and G. Drettakis, "3d gaussian splatting for real-time radiance field rendering," *ACM Trans. Graph.*, vol. 42, no. 4, pp. 139–1, 2023.
- [4] X. Wang, W. Zhang, H. Xie, H. Ai, Q. Yuan, and Z. Zhan, "Tortho-gaussian: Splatting true digital orthophoto maps," *arXiv preprint arXiv:2411.19594*, 2024.
- [5] J. Yang, Z. Cai, T. Wang, T. Ye, H. Gao, and H. Huang, "Ortho-3dgs: True digital orthophoto generation from unmanned aerial vehicle imagery using the depth-regulated 3d gaussian splatting," *IEEE Journal of Selected Topics in Applied Earth Observations and Remote Sensing*, 2025.
- [6] D. Wei and G. Zhou, "Real-time uav ortho video generation," in *IGARSS 2008-2008 IEEE International Geoscience and Remote Sensing Symposium*, vol. 5. IEEE, 2008, pp. V-510.
- [7] T. Hinzmann, J. L. Schönberger, M. Pollefeys, and R. Siegwart, "Mapping on the fly: Real-time 3d dense reconstruction, digital surface map and incremental orthomosaic generation for unmanned aerial vehicles," in *Field and Service Robotics: Results of the 11th International Conference*. Springer, 2017, pp. 383–396.
- [8] B. Du, H. Ye, Y. Zhang, and X. Liao, "A real-time orthophoto generation approach for uav based on deep learning visual feature," *IEEE Transactions on Geoscience and Remote Sensing*, 2025.
- [9] Z. Zhan, Y. Yu, R. Xia, *et al.*, "Sfm on-the-fly: Get better 3d from what you capture," *ISPRS Journal of Photogrammetry and Remote Sensing*, vol. 224, pp. 202–221, 2025.
- [10] Y. Xu, Y. Yu, W. Gan, T. Wang, Z. Zhan, H. Cheng, and X. Wang, "Gaussian on-the-fly splatting: A progressive framework for robust near real-time 3dgs optimization," *arXiv preprint arXiv:2503.13086*, 2025.
- [11] S. Bu, Y. Zhao, G. Wan, and Z. Liu, "Map2dfusion: Real-time incremental uav image mosaicing based on monocular slam," in *2016 IEEE/RSJ International Conference on Intelligent Robots and Systems (IROS)*. IEEE, 2016, pp. 4564–4571.